Possible spin triplet superconductivity in $Na_xCoO_2 \cdot yH_2O$ — ^{59}Co NMR studies

2006 J. Phys.: Condens. Matter 18 669

(http://iopscience.iop.org/0953-8984/18/2/022)

INSTITUTE OF PHYSICS PUBLISHING JOURNAL OF PHYSICS: CONDENSED MATTER

J. Phys.: Condens. Matter **18** (2006) 669–682 doi:10.1088/0953-8984/18/2/022

Possible spin triplet superconductivity in $Na_xCoO_2{\cdot}yH_2O$—^{59}Co NMR studies

M Kato[1,5], C Michioka[1], T Waki[1], Y Itoh[1], K Yoshimura[1], K Ishida[2], H Sakurai[3], E Takayama-Muromachi[3], K Takada[4] and T Sasaki[4]

[1] Department of Chemistry, Graduate School of Science, Kyoto University, Kyoto 606-8502, Japan
[2] Department of Physics, Graduate School of Science, Kyoto University, Kyoto 606-8502, Japan
[3] Superconducting Materials Centre, National Institute for Materials Science, 1-1 Namiki, Tsukuba, Ibaraki 305-0044, Japan
[4] Advanced Materials Laboratory, National Institute for Materials Science, Namiki 1-1, Tsukuba, Ibaraki 305-0044, Japan

E-mail: makato@mail.doshisha.ac.jp

Received 8 November 2005
Published 14 December 2005
Online at stacks.iop.org/JPhysCM/18/669

Abstract

We report ^{59}Co NMR studies on magnetically oriented powder samples of Co oxide superconductors, $Na_xCoO_2{\cdot}yH_2O$, with $T_c \sim 4.7$ K. From the two-dimensional powder pattern in the NMR spectrum, the ab-plane Knight shift in the normal state was estimated from the magnetic field dependence of the second-order quadrupole shifts at various temperatures. Below 50 K, the Knight shift shows a Curie–Weiss-like temperature dependence, similarly to the bulk magnetic susceptibility χ. From the analysis of the so-called $K-\chi$ plot, the spin and the orbital components of K and the positive hyperfine coupling constant were estimated. The onset temperature of the superconducting transition in the Knight shift does not change much in an applied magnetic field up to 7 T, which is consistent with the reported high upper critical field H_{c2}. The Knight shift at 7 T shows an invariant behaviour below T_c. No coherence peak just below T_c was observed in the temperature dependence of the nuclear spin–lattice relaxation rate $1/T_1$ in either case (NMR, nuclear quadrupole resonance). We conclude that the invariant behaviour of the Knight shift below T_c and unconventional behaviours of $1/T_1$ may indicate spin triplet superconductivity with p- or f-wave symmetry.

1. Introduction

The recent discovery of superconductivity in $Na_xCoO_2{\cdot}yH_2O$ with a transition temperature (T_c) of about 4.7 K [1] has been a major breakthrough in the search for novel layered

[5] Present address: Department of Molecular Science and Technology, Faculty of Engineering, Doshisha University, Kyotanabe, Kyoto 610-0394, Japan.

0953-8984/06/020669+14$30.00

transition metal oxide superconductors. $Na_xCoO_2 \cdot yH_2O$ has a two-dimensional (2D) crystal structure where Co atoms form a 2D triangular lattice separated by Na^+ ions and H_2O molecules. The intercalation of H_2O molecules leads to an increase of the c-axis lattice constant, which is considered to enhance the two dimensionality of the CoO_2 layers. The triangular configuration on the CoO_2 plane potentially has the possibility for exhibiting unconventional superconductivity via a highly fortuitous mechanism in the novel quantum state, as suggested by many theoretical works. For example, Tanaka *et al* indicated that the spin triplet superconductivity may be realized with a pairing process similar to that of Sr_2RuO_4, since the hexagonal structure in $Na_xCoO_2 \cdot yH_2O$ is favoured for a spin triplet pairing [2]. Some groups studied a single-band t–J model as a prototype for strong coupling electron theories in an effort to understand the low energy electronic phenomena on the basis of the resonating-valence-bond (RVB) state [3–7]. Kuroki *et al* introduced a single-band effective model taking into account pocket-like Fermi surfaces along with van Hove singularity near the K point in the first Brillouin zone [8–11]. They showed that the large density of states near the Fermi level gives rise to ferromagnetic spin fluctuations, leading to f-wave superconductivity due to disconnected Fermi surfaces near the Γ point. Khaliullin *et al* emphasized the importance of a spin–orbit (LS) coupling, and showed that the hole carriers with pseudo-spin one-half on an f level, separated from t_{2g} orbital degeneracy due to trigonal distribution and spin–orbit interaction, make the spin triplet state always favoured [12].

In order to clarify the superconducting mechanism in $Na_xCoO_2 \cdot yH_2O$, it is very important to investigate the Cooper-pair symmetry. Nuclear magnetic resonance (NMR) is known as a powerful probe for investigating the pairing symmetry in the superconducting state. In this paper, we report detailed experimental results on the Knight shift, K, and the spin–lattice relaxation rate, $1/T_1$, of $Na_xCoO_2 \cdot yH_2O$ obtained by means of ^{59}Co NMR and nuclear quadrupole resonance (NQR) measurements. We demonstrate that K_y, one of the in-plane Knight shifts, is invariant below T_c at a high field of about 7 T, where $1/T_1$ drops at T_c and obeys a T^3 law without a coherence peak just below T_c. These results are attributable to the possible formation of p- or f-wave superconducting states with line nodes in the superconducting gap. Our results are inconsistent with the previous report by Kobayashi *et al*, which suggested spin singlet s-wave superconductivity from the results at a lower field of about 2 T [13]. However, the precise values of the Knight shift cannot be estimated without explaining the frequency dependence of the field-swept spectra because of the coexistence of electric quadrupole and Zeeman interactions. Thus, we clearly present how to estimate the spin part of the Knight shift using the frequency dependence of resonance fields above T_c. The full analysis of the NMR parameters is crucially important for discussing the Cooper-pair symmetry in the superconducting state.

2. Experiments

The powder sample of $Na_xCoO_2 \cdot yH_2O$ was prepared by an oxidation process from the mother compound, $Na_{0.7}CoO_2$ [1]. The sample obtained was confirmed to be a single phase by powder x-ray diffraction (XRD) measurements. The chemical contents of Na and H_2O were found to be about 0.35 and 1.3, respectively, by inductively coupled plasma atomic emission spectroscopy (ICP) [1]. The superconducting transition temperature (T_c) was estimated from the temperature dependence of the magnetization using a SQUID magnetometer. ^{59}Co NMR and NQR measurements were performed by the spin echo method with a standard phase coherent-type pulsed spectrometer. The powder sample was oriented and fixed by using an organic solvent, hexane, under conditions with an external field $H = 8$ T. In our NMR measurement, hexane was found to be an optimal agent for fixing the sample because it has the

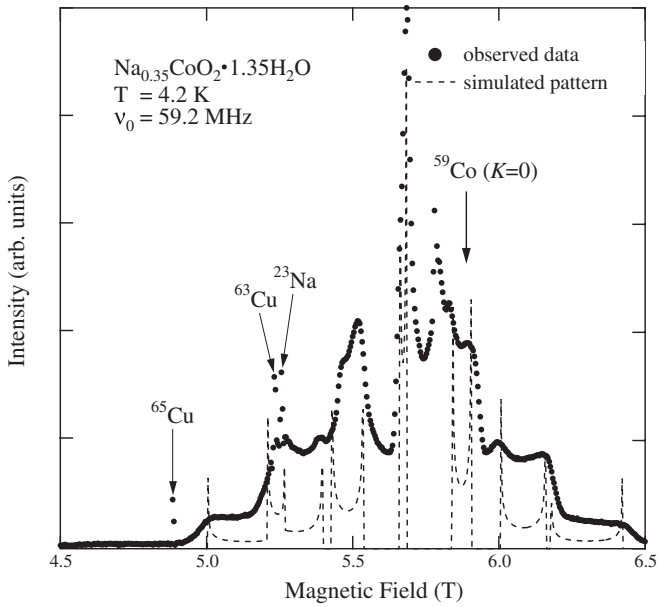

Figure 1. Field-swept NMR spectrum of $Na_xCoO_2 \cdot yH_2O$ at a constant frequency (ν_0) of 59.2 MHz taken at 4.2 K. Arrows indicate the resonance fields of ^{63,65}Cu nuclei in the resonance coil, ^{23}Na nuclei and the Knight shift reference position ($K = 0$) of ^{59}Co nuclei. Filled circles show the observed data. The dashed line indicates the peak positions and intensities simulated for the case of an anisotropic Knight shift and a second-order quadrupole effect with $K_x = 3.56\%$, $K_y = 3.21\%$, $\nu_Q = 4.15$ MHz and the asymmetric parameter of the electric field gradient $\eta = 0.21$.

melting point of 178 K and does not absorb water molecules. Stycast 1266, which is useful for high T_c cuprate superconductor studies, was not suitable owing to its desiccating effect. From the XRD measurement, we found that the c-axis of the sample was oriented perpendicular to the external magnetic field H and that the random orientation in the c-plane was obtained along H. Since the orientation and the NMR measurements were performed at the same time, the magnetic field in the NMR was applied in completely the same direction as that of the sample alignment. NQR measurements were performed in zero field. $1/T_1$ was estimated by monitoring the recovery of the spin echo amplitude, $M(t)$, after an inversion pulse, as a function of the delay time (t) between the inversion π and the observation radio-frequency $\pi/2-\pi$ pulses.

Once the sample was cooled, it was kept below 100 K even during the intermissions between NMR and NQR measurements. We must maintain the orientation throughout the measurements because the resonance fields for peaks and shoulders of the NMR spectrum are sensitive to the sample orientation. We also notice that it is extremely important to avoid a shortage of H_2O molecules since the superconducting properties such as T_c are sensitive to the H_2O content [14].

3. Results and discussion

3.1. ^{59}Co Knight shift above T_c

Figure 1 shows a typical ^{59}Co NMR spectrum of $Na_xCoO_2 \cdot yH_2O$ at a frequency of 59.200 MHz. The observed NMR spectrum can be understood via a 2D powder pattern with anisotropic

Knight shifts and the second-order quadrupole interaction. We have succeeded in determining these NMR parameters from the following analysis.

In order to determine the Knight shift above T_c, we use the central transition line ($+1/2 \leftrightarrow -1/2$) as shown in figure 2. We assume that the principal axes of the Knight shift tensor coincide with those of the electric field gradient (EFG) tensor. This assumption is generally rational because those tensors are mainly governed by the local symmetry around the Co site. Because of the quadrupole effect up to the second-order perturbation, a conventional 3D powder pattern of the central transition has five specific resonance frequencies ν_1–ν_5 in a constant field which are equivalent to the resonance fields H_1–H_5 at a constant frequency (ν_0) [15]. These fields can be observed as two peaks (H_2 and H_4), two shoulders (H_1 and H_5) and a step (H_3) in the case of $\eta < \frac{1}{3}$, where η is the asymmetric parameter of the EFG tensor defined by $\eta = |V_{XX} - V_{YY}|/|V_{ZZ}|$, in which V_{ii} ($ii = XX, YY, ZZ$) are the principal components of the EFG tensor with the relation $|V_{XX}| \leqslant |V_{YY}| \leqslant |V_{ZZ}|$ [15]. In the present case of the 2D powder spectrum, only two peaks appear at specific resonance fields (H_1 and H_2) because of the sample orientation. Hence the central spectrum should consist of two peaks at H_1 and H_2. Actually, the central resonance was decomposed into two Gaussian components using least-squares fitting to determine the experimental values of H_1 and H_2, as shown in figure 2. These resonance fields at a constant frequency ν_0 are expressed using K_j, principal values of the Knight shift tensor, and ν_Q, the quadrupole frequency, as follows:

$$\frac{\delta\nu_i}{\gamma_N H_i} = K_j + \frac{C_i}{(1+K_j)(\gamma_N H_i)^2}, \tag{1}$$

$$\delta\nu = \nu_0 - \gamma_N H_i, \tag{2}$$

$$C_1 = \frac{R(3+\eta)^2}{144}, \qquad C_2 = \frac{R(3-\eta)^2}{144}, \tag{3}$$

$$R = \nu_Q^2[I(I+1) - \tfrac{3}{4}], \tag{4}$$

where the values with $j = X, Y$ correspond to those with $i = 1, 2$, respectively, γ_N is the nuclear gyromagnetic ratio (10.054 MHz T^{-1} for ^{59}Co with the nuclear spin of $I = 7/2$) [15]. As seen in equation (1), a linear relation should be expected when $\delta\nu_i/\gamma_N H_i$ is plotted against $(\gamma_N H_i)^{-2}$. Then, the intercepts on the vertical axis at $(\gamma H_i)^{-2} \to 0$ give the values of K_x and K_y independently of ν_Q.

Figure 3 shows the experimental values of $\delta\nu/(\gamma_N H_i)$ plotted against $(\gamma_N H_i)^{-2}$ ($i = 1, 2$) measured above T_c and at 4.2 K in the frequency range of 44.2–74.2 MHz. This plot is referred to as a second-order quadrupole plot. The experimental values of $\delta\nu_i/\gamma H_i$ clearly lie on the respective straight lines against $(\gamma H_j)^{-2}$ in the plots. One should note that K_x and K_y (intercepts of the $\delta\nu_i/\gamma_N H_i$ axis) decrease with heating while the slopes are almost independent of T. Since the slope of the line $C_i/(1+K_j)$ ($\simeq C_i$) is determined by ν_Q and η, the almost invariant slope indicates that ν_Q and η are almost constant in this temperature range. This result is consistent with our NQR experiment (not shown here). The inset in figure 3 shows the result of the least-squares fitting using equations (1)–(4) at 4.2 K. The NMR parameters obtained are $K_x = 3.56\%$, $K_y = 3.21\%$, $\nu_Q = 4.15$ MHz and $\eta = 0.21$. These parameters were estimated at other temperatures similarly. Using these parameters, we can calculate the simulated spectra as shown by the dashed lines in figure 1. Consequently, the simulated spectrum including first, second and third satellites is in good agreement with the observed one.

Within the analysis mentioned above, we could not estimate the Z component of the Knight shift due to the 2D sample orientation. However, we have estimated this value as follows. In figure 1, we noticed a peak at around $H = 5.8$ T, which is not usually expected for the 2D pattern. We regarded this peak as the NMR signal from the accidentally aligned powders along

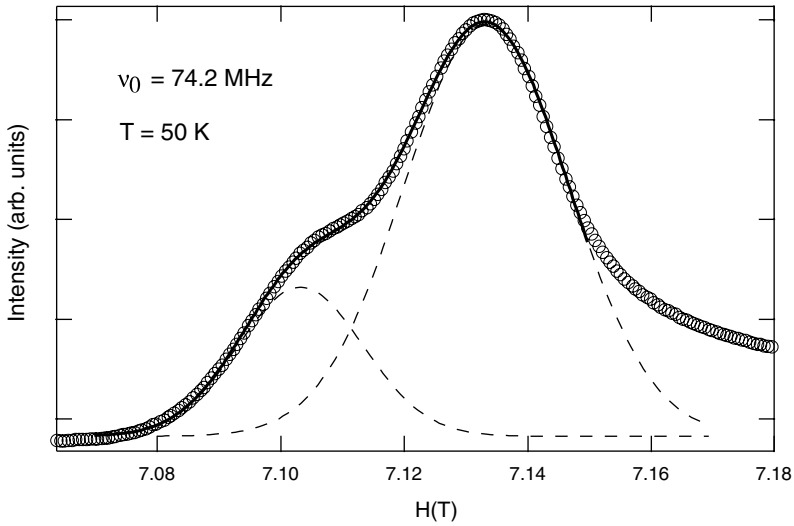

Figure 2. Field-swept NMR spectrum of $Na_{0.35}CoO_2 \cdot 1.3H_2O$ at $T = 50$ K and $\nu_0 = 74.2$ MHz. Two peaks, which are decomposed by the Gaussian fitting indicated by the dashed lines, correspond to the central resonance of the $I_z = -1/2 \leftrightarrow 1/2$ transition. The anisotropic Knight shifts K_x and K_y were estimated from the low field smaller peak and the high field larger peak, respectively (see the text).

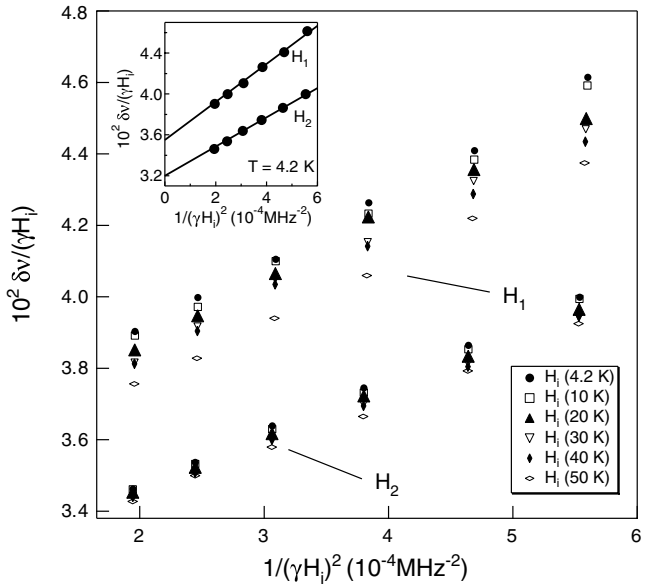

Figure 3. Second-order quadrupole plot for various temperatures above T_c and 4.2 K (just below T_c) obtained for ν_0 ranging from 44.2 to 74.2 MHz. H_1 and H_2 are the resonance fields at which the ^{59}Co NMR spectrum with the 2D powder pattern of the central transition shows two singular points. The inset shows the data at 4.2 K with the fitted lines obtained using the NMR parameters, $\nu_Q = 4.15$ MHz, $\eta = 0.21$, $K_x = 3.56\%$ and $K_y = 3.21\%$.

the c-axis. Assuming that this peak corresponds to H_3, another step in the powder spectrum (a peak in the c-axis oriented spectrum), we have estimated the value of $K_z = 1.88\%$.

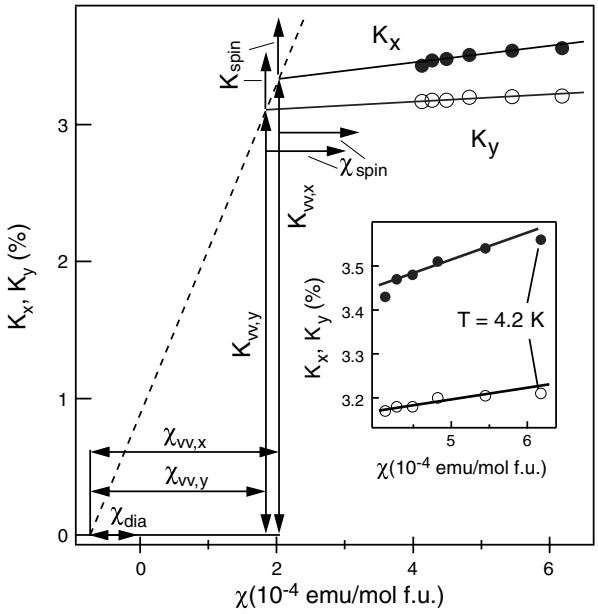

Figure 4. Knight shift versus susceptibility diagram for $Na_{0.35}CoO_2{\cdot}1.3H_2O$. The data at 4.2 K (below T_c) are shown for comparison but not used for the line fitting. The inset shows the expansion. The numerical details for constructing the diagram are given in the text. The dashed line is the orbital shift against the orbital susceptibility, $K_{VV} = A_{hf}^{VV} \times \chi_{VV}$.

In figure 4, we indicate the K_x and K_y obtained against the uniform magnetic susceptibility with temperature as an implicit parameter. This is a so-called K–χ plot, which is useful for the analysis of various contribution to the Knight shift [16]. For the 3d transition metal oxides, the Knight shift can be expressed by

$$K(T) = K_{spin}(T) + K_s + K_{VV}, \tag{5}$$

where $K_{spin}(T)$, K_s and K_{VV} are a T dependent spin shift, a T independent spin shift and a Van Vleck orbital shift, respectively. The magnetic susceptibility can be expressed by

$$\chi(T) = \chi_{spin}(T) + \chi_s + \chi_{VV} + \chi_{dia}, \tag{6}$$

where $\chi_{spin}(T)$, χ_s, χ_{VV} and χ_{dia} are a T dependent spin susceptibility, a T independent spin susceptibility, a Van Vleck orbital susceptibility and a diamagnetic susceptibility of core electrons, respectively. The hyperfine coupling constants connect the respective components of the ^{59}Co Knight shift in equation (5) to those of the magnetic susceptibilities in equation (6) as follows:

$$K_{spin}(T) = A_{hf}\chi_{spin}(T), \tag{7}$$

$$K_s = A_s\chi_s, \tag{8}$$

$$K_{VV} = A_{VV}\chi_{VV}. \tag{9}$$

The diamagnetic susceptibilities of core electrons can be estimated from relativistic Hartree–Fock calculations. From $\chi_{dia}^{H} = -0.4\times10^{-9}\,\mu_B$/atom, $\chi_{dia}^{O} = -1.6\times10^{-9}\,\mu_B$/atom, $\chi_{dia}^{Na} = -3.8\times10^{-9}\,\mu_B$/atom and $\chi_{dia}^{Co} = -5.5\times10^{-9}\,\mu_B$/atom [17], the total diamagnetic susceptibility of $Na_xCoO_2{\cdot}yH_2O$ was estimated to be $\chi_{dia} = 7.3\times10^{-5}$ emu mol^{-1}. The hyperfine coupling constant for the d orbital Van Vleck component, $A_{hf}^{VV} = K_{VV}/\chi_{VV} =$

6.7×10^2 kOe μ_B^{-1} was assumed, using $2/\langle r^{-3}\rangle = 9.05\times10^{25}$ cm^{-3} for Co^{3+} and the reduction factor of 0.8 for the metallic state compared with the free ion. Using these parameters, the coupling constants for the temperature dependent Knight shift components, A_{hf}^x and A_{hf}^y, were estimated to be +34 and +14.7 kOe μ_B^{-1} by the least-squares fitting shown with solid lines in figure 4. Then, $\chi_{VV,x}$ and $\chi_{VV,y}$ were estimated to be 2.0×10^{-4} and 1.8×10^{-4} emu mol^{-1} fu^{-1}, respectively, and $K_{VV,x}$ and $K_{VV,y}$ to be 3.3% and 3.1%, respectively, at most. Therefore the spin Knight shifts were found to be ∼0.3% for K_x and ∼0.1% for K_y at least.

The hyperfine constant of coupling between the Co nuclear spin and the electron spins, A_{hf}, can be expressed by

$$A_{hf} = A_{cp} + A_{dip} + A_{orb} + A_{tr}, \tag{10}$$

where the on-site hyperfine coupling constants A_{cp}, A_{dip} and A_{orb} originate from the core polarization, dipolar interaction and spin–orbit coupling, respectively, and A_{tr} is from the supertransferred hyperfine field. For 3d transition metals, the hyperfine coupling constant due to the core spin polarization of 3d electrons is *negative* with $A_{cp} \approx -100$ kOe μ_B^{-1} [18]. The observed *positive* hyperfine coupling constant of $Na_{0.35}CoO_2{\cdot}1.3H_2O$ is unusual. For some Co oxides [19–21] and alloys [22, 23], the *positive* hyperfine coupling constant of ^{59}Co nuclei was observed and attributed to the presence of a large LS coupling effect. In the present case, a large orbital contribution to K_{spin} via the LS coupling can account for the *positive* A_{hf}.

In our preliminary experiment, for a nonoriented 3D powder sample, K_z is also estimated to be positive, ∼1.88%. The positive coupling constant is probably caused by not only the anisotropic A_{orb} and A_{dip} but also the transferred hyperfine field A_{tr}. At the present stage, we cannot estimate A_{orb} and A_{tr} separately. The value of K_y is consistent with that reported by Mukhamedshin *et al* [24].

At first, in the analysis in figure 4, we assumed the temperature independent Knight shift to be K_{VV}. However, we must consider the possibility that a part of the spin term does not depend on temperature and that K_{VV} may be smaller than the estimated value, which should be important when two bands are dominant in the Fermi surface. That is, there must be a finite contribution of K_s in equation (5) and χ_s in equation (6).

3.2. ^{59}Co Knight shift below T_c

Figure 5 shows the temperature dependence of the central spectra at a higher field (about 7 T). Since the estimated upper critical field H_{c2} of $Na_xCoO_2{\cdot}yH_2O$ was reported to be high, 61 T from the magnetization measurement [25] and 17.1 T from the heat capacity measurement [26], it should be noted that T_c is almost constant, and that samples were in the superconducting state below T_c in our experimental conditions. As seen in figure 5, the central resonance fields H_1 and H_2 above T_c shift to higher values with increasing temperature, suggesting that the spin contributed Knight shift increases owing to the positive hyperfine coupling constants with a second-order quadrupole shift as discussed above. On the other hand, the values of H_1 and H_2 do not change below T_c, indicating that K_x and K_y are almost constant at 3.56 and 3.21% below T_c under a field of about 7 T within experimental precision. In the BCS theory, the spin susceptibility, χ_{spin}, in the superconducting state is described as

$$\chi_{spin} = -4\mu_B^2 \int_0^\infty N_s(E)\frac{\partial f(E)}{\partial E}\,\mathrm{d}E, \tag{11}$$

where μ_B is the Bohr magneton, $N_s(E)$ is the quasiparticle density of states and $f(E)$ is the Fermi–Dirac distribution function. It is widely known for a singlet pairing superconductor that the spin Knight shift decreases with cooling and vanishes at $T = 0$ in the Yosida function, being proportional to $e^{-\Delta(0)/kT}$ at $T \ll T_c$ [27]. The mean free path l is estimated to be

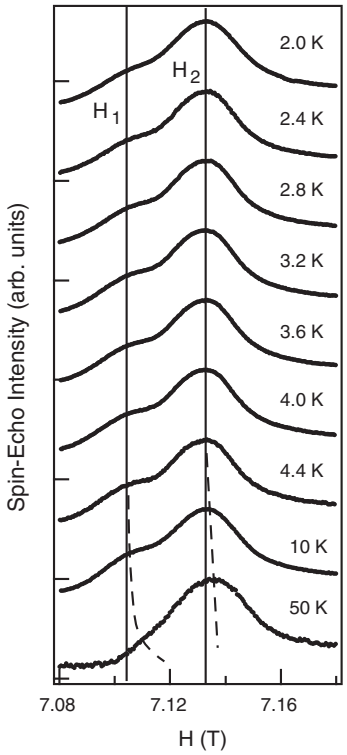

Figure 5. Temperature dependence of the central resonance in the spin echo spectra at ν_0 of 74.2 MHz. Solid lines and dashed curves are guides for the eyes. The central resonance field does not change below T_c.

$l \geqslant 100$ Å from the low temperature resistivity [28] and the Fermi wavenumber k_F [29], and the coherence length ξ to be $\xi \sim 23.2$ Å [25]. Since the l/ξ ratio is larger than 4, this system can be considered to be a clean superconductor. Thus, the invariant behaviour of K_x and K_y at about 7 T suggests a spin triplet p- or f-wave pairing superconductivity.

Figure 6 shows the central peaks in the field-swept spectra at 2.0 and 4.2 K at several constant frequencies (44.2–74.2 MHz). The resonance fields are almost the same between 2.0 and 4.2 K at $\nu_0 = 74.2$ MHz, but change drastically at $\nu_0 = 44.2$ MHz. The difference of the resonance fields between 2.0 and 4.2 K gradually increases with decreasing experimental frequency. As well as that for the normal state, we discuss the second-order quadrupole plot for the superconducting state, shown in figure 7. Only H_2 was estimated from the peaks in the spectra, because it was difficult to decompose the spectra, especially at lower frequencies. In figure 7, the experimental values at 4.4 K show a linear relation similar to those above T_c in figure 3. On the other hand, the slope for the superconducting state seems to decrease with temperature, that is, a nonlinear relation appears below T_c. Since ν_Q and η are almost constant also below T_c, as was confirmed by our NQR measurements, the decrease of the slope is not due to the change in the quadrupole shift below T_c. Thus, the Knight shift itself must depend on the applied magnetic field.

In figure 8, we estimate the temperature dependence of the spin part of the ^{59}Co Knight shift at various resonance frequencies ν_0 below T_c and the Knight shift of ^{23}Na nuclei. This estimation was done by extrapolating from the respective data points in the second-order

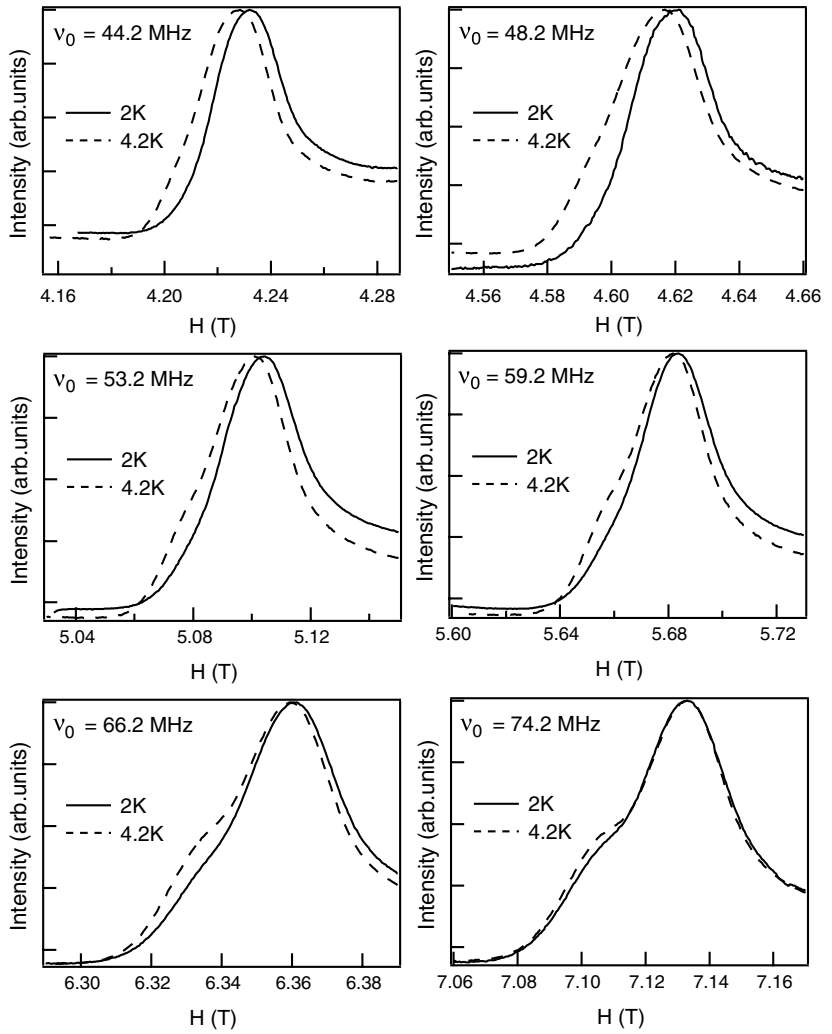

Figure 6. Field-swept 2D powder spectra for the central transitions at 2.0 and 4.2 K taken at several fixed frequencies, ν_0.

quadrupole plot in figure 7 and equation (1), assuming that all the slopes, C_i in equation (1), were fixed at the same value at 4.2 K. As shown in figure 8, the temperature dependent term of the shift increases with decreasing ν_0. One should note that the values of the T_c onsets are almost invariant with changing magnetic field, which is consistent with the rather high value of H_{c2}. The behaviour of the Knight shift below T_c can be explained by a superconducting diamagnetic shift or a field-induced spin Knight shift.

At first we discuss the possibility of a site dependent diamagnetic effect. The Knight shift of ^{23}Na does not change with $K \sim 0$, indicating that the spin contribution is small and the diamagnetic shift in the superconducting state is also small. The effect of the diamagnetic shift was remarkable at the ^{59}Co nuclear sites but negligible at the ^{23}Na sites. If Josephson vortices penetrated into the Na layers, the diamagnetic shift due to supercurrents would be expected to be large at the Co sites but not at the Na site. Theoretically, in the vortex state with an extremely

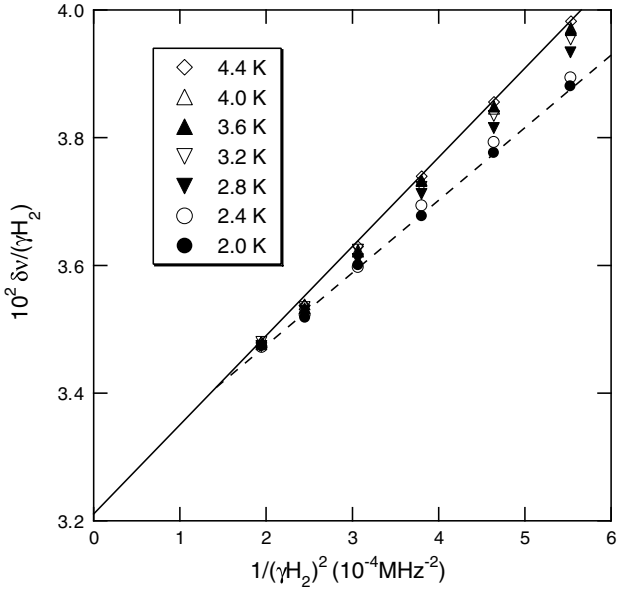

Figure 7. Second-order quadrupole plots for H_2 at various temperatures below T_c. The solid line is the same as the one for H_2 shown in the inset of figure 3. The dashed line is a guide for the eyes. The slope of the linear correlation seems to change below T_c. This is not due to the change of ν_Q or that of η, but may be due to the diamagnetic effect.

strong two-dimensional system, that is, with a short coherence length along the c-axis, the layer itself works as strong pinning centres for the vortices, resulting in the diamagnetic effect possibly depending on the sites in a unit cell [30]. Although for $Na_{0.35}CoO_2{\cdot}1.3H_2O$ no direct evidence of intrinsic pinning was obtained, the Josephson vortex can be expected because of the strong two-dimensionality of this compound. Thus the invariant behaviour of the Knight shift at about 7 T should be intrinsic, suggesting spin triplet superconductivity.

If the change of the resonance fields below T_c at low fields shown in figure 6 is not attributable to the diamagnetic effect but due to the change of the intrinsic spin shift, the spin shift decreases with decreasing temperature. In this case, the spin triplet superconductivity with the superconducting d-vector perpendicular to the c-axis as well as the case of the spin singlet superconductivity can be considered. Recent theoretical study suggested that the hole pocket near the K point leads to ferromagnetic fluctuation, resulting in a spin triplet p- or f-wave superconductivity with the d-vector pointing perpendicularly to the c-axis in the presence of the strong spin–orbit coupling [31, 32]. A part of the in-plane spin shift perpendicular to the d-vector may be suppressed at $T = 0$ K. The magnetic field induces a local density of states around the vortex cores, and then a part of the in-plane shift recovers. In this case, the key point is the Knight shift along the c-axis, K_z. In the preliminary results obtained using the resonance centre, which is due to the accidental alignment along the c-axis already mentioned, the temperature dependence of K_z above T_c should be very small, suggesting a small contribution of the spin shift, and at least that K_z does not change below T_c.

3.3. ^{59}Co nuclear spin–lattice relaxation time T_1

We measured $1/T_1$ for ^{59}Co under the central resonance field at the frequency of H_2 in order to obtain information on the low lying quasiparticle states below and above T_c. In figure 9, we

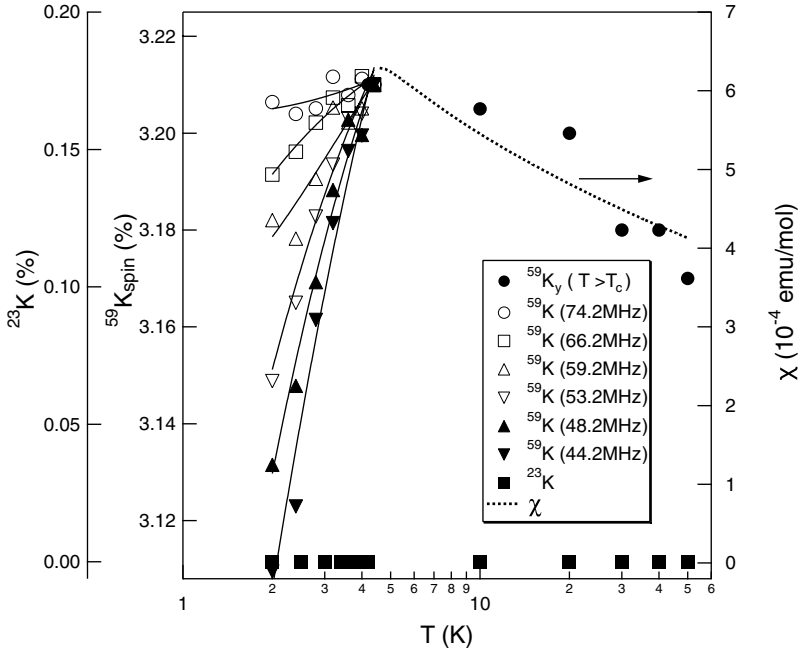

Figure 8. Temperature dependence of the estimated spin part of the Knight shift at various resonance frequencies ν_0. The K_y data below T_c were obtained by extrapolation from the respective data points in figure 7 and equation (1) assuming that ν_Q and η, and thus C_i in equation (1), are the same as those at 4.2 K. Here, a dashed line indicates the temperature dependence of χ. Solid lines are guides for the eyes.

show recovery curves at 4.2 K measured using NQR and NMR (at H_2) methods. The recovery curves for NQR signals at 4.2 K were analysed using the same function as was reported in [33] and [34]. In the case of NMR, the observed recovery curves were found to consist of more than one relaxation component, perhaps due to the overlap of satellite resonances in the powder spectrum. Thus, we should utilize a combination of the theoretical relaxation function for the central resonance and a slow single-exponential component, as follows:

$$\frac{M(\infty) - M(t)}{M(\infty)} = A\left(\frac{1}{84}e^{\frac{-t}{T_1}} + \frac{3}{44}e^{\frac{-6t}{T_1}} + \frac{75}{364}e^{\frac{-15t}{T_1}} + \frac{1225}{1716}e^{\frac{-28t}{T_1}}\right) + Be^{\frac{-t}{T_1^{\text{slow}}}}, \tag{12}$$

where A, B, T_1 and T_1^{slow} are fitting parameters. The solid lines in figure 9 are the results of the least-squares fitting using equation (12). The extrinsic slow component was very small; $B/(A + B)$ was found to be about 0.8%. Figure 10 shows the temperature dependence of $1/T_1T$ and the inset of the figure shows that of $1/T_1T$. In NQR measurements, $1/T_1$ rapidly decreases with temperature below T_c with a T^3 dependence. This result is consistent with the data previously reported [33, 34].

Under the field of 7.12 T, a rapid decrease in $1/T_1T$ is also observed below 4.4 K, which indicates that T_c does not decrease markedly under the external field. We would like to note that H_{c2} under a magnetic field parallel to the CoO_2 plane is quite large and T_c decreases very little (estimated as only about 0.3 K smaller than that at zero field) at about 7 T. It is also noted that another enhancement of $1/T_1T$ below T_c occurs, which may suggest the presence of an unconventional vortex state because this behaviour cannot be observed in the NQR measurement under zero magnetic field.

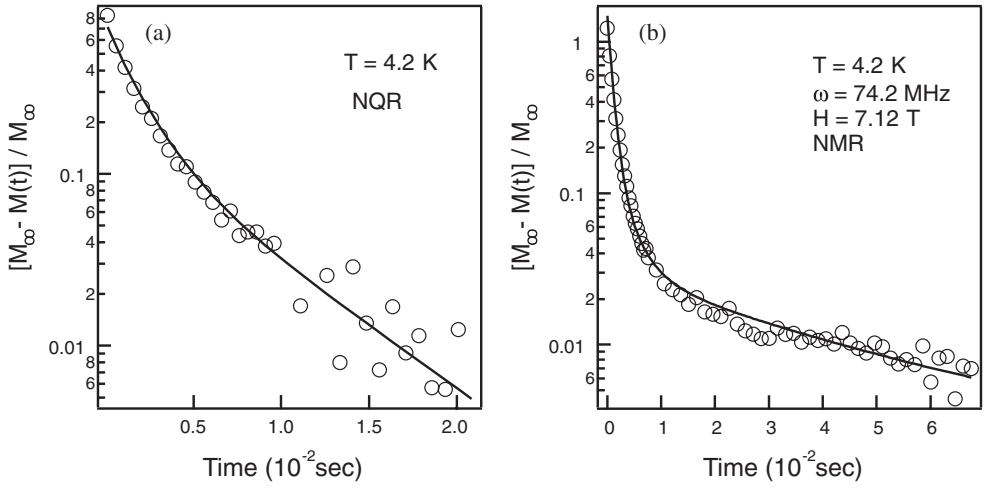

Figure 9. Recovery curves at 4.2 K (a) for the highest frequency transition of ^{59}Co NQR and (b) the centre transition of the NMR taken at 74.2 MHz. The values of $1/T_1$ were estimated by least-squares fitting (see the text).

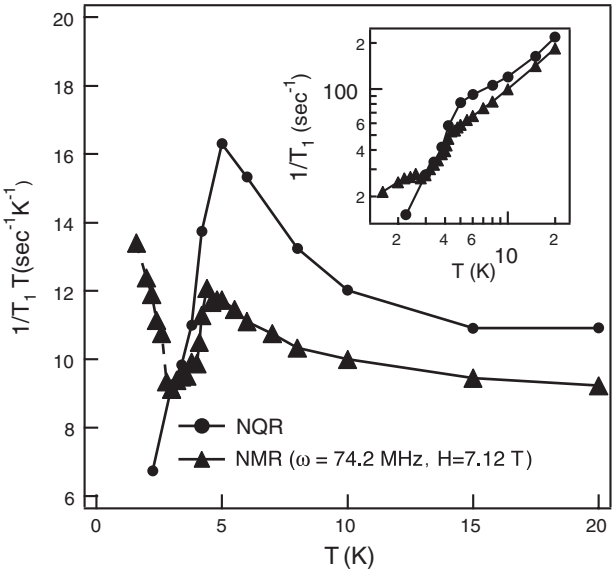

Figure 10. Temperature dependence of $1/T_1T$ for $Na_xCoO_2{\cdot}yH_2O$. Filled circles are from the ^{59}Co NQR data at zero external field and triangles are those from the NMR at 7.12 T. The inset shows the temperature dependence of $1/T_1$. One can note that $1/T_1$ decreases proportionally to T^3 just below T_c even under $H = 7$ T.

The T^3 dependence of $1/T_1$ below T_c without any coherence peaks indicates the presence of line nodes on the Fermi surface. A recent study on the mother compound Na_xCoO_2 revealed that the ferromagnetic spin fluctuations are dominant in the magnetism on the CoO_2 plane [36]. For our hydrated $Na_xCoO_2{\cdot}yH_2O$, one should note in figure 10 that the enhancement of $1/T_1T$ in the NQR just above T_c is suppressed at 7.12 T, which indicates that the ferromagnetic fluctuation is dominant in the same temperature range, as also suggested by the enhancement

of the magnetic susceptibility in figure 8. This situation could be suitable for the occurrence of spin triplet superconductivity.

4. Summary

From the analysis of the temperature dependence of the field-swept NMR spectra, we estimated the spin component of the ^{59}Co Knight shift of $Na_xCoO_2 \cdot yH_2O$. For the normal state, the in-plane spin Knight shifts were found to be proportional to χ and to have values of 0.3 and 0.1% for K_x and K_y at least just above T_c. In the superconducting state, the intrinsic Knight shift does not change with temperature at the external field of about 7 T, much smaller than H_{c2}, although the Knight shift is not estimated correctly at lower fields because of a lack of information on the precise diamagnetic effects. We emphasize that the invariant behaviour of the Knight shift in higher fields is consistent with that in μSR experiments [35]. From these results, we conclude that the p- or f-wave pairing state with triplet spin symmetry may be the most preferred in the superconducting state of $Na_xCoO_2 \cdot yH_2O$.

Acknowledgments

This study was supported by a Grant-in-Aid on the priority area 'Novel Quantum Phenomena in Transition Metal Oxides', from the Ministry of Education, Science, Sports and Culture (12046241, 16076210), and also supported by a Grant-in-Aid for Scientific Research from the Japan Society for Promotion of Science (14654060, 14740382, 17750059).

References

[1] Takada K, Sakurai H, Takayama-Muromachi E, Izumi F, Dilanian R A and Sasaki T 2003 *Nature* **422** 53
[2] Tanaka A and Hu X 2003 *Phys. Rev. Lett.* **91** 257006
[3] Anderson P W 1973 *Mater. Res. Bull.* **8** 153
[4] Baskaran G 2003 *Phys. Rev. Lett.* **91** 097003
[5] Kumar B and Shastry B S 2003 *Phys. Rev.* B **68** 104508
[6] Wang Q H, Lee D H and Lee P A 2004 *Phys. Rev.* B **69** 092504
[7] Ogata M 2003 *J. Phys. Soc. Japan* **72** 1839
[8] Kuroki K, Tanaka Y and Arita R 2004 *Phys. Rev. Lett.* **93** 077001
[9] Arita R, Kuroki K and Aoki H 1999 *Phys. Rev.* B **60** 14585
[10] Kuroki K and Arita R 2001 *Phys. Rev.* B **63** 174507
[11] Kuroki K and Arita R 2001 *Phys. Rev.* B **64** 024501
[12] Khaliullin G, Koshibae W and Maekawa S 2004 *Phys. Rev. Lett.* **93** 176401
[13] Kobayashi Y, Yokoi M and Sato M 2003 *J. Phys. Soc. Japan* **72** 2453
[14] Ohta H, Michioka C, Itoh Y and Yoshimura K 2005 *J. Phys. Soc. Japan* **74** 3147
[15] Baugher J F, Taylor P C, Oja T and Bary P J 1969 *J. Chem. Phys.* **50** 4914
[16] Seitchik J A, Gossard A C and Jaccarino V 1964 *Phys. Rev.* A **4** A1119
[17] Mendelsohn L B, Biggs F and Mann J B 1970 *Phys. Rev.* A **2** 1130
[18] Freeman A and Watson R E 1965 Hyperfine interactions in magnetic materials *Magnetism* ed T Rado and H Suhl (New York: Academic)
[19] Itoh M and Natori I 1995 *J. Magn. Magn. Mater.* **140–144** 2145
[20] Miyatani K, Korn K, Kamimura E and Iida S 1966 *J. Phys. Soc. Japan* **21** 464
[21] Hayakawa Y, Kohiki S, Sato M, Sonoda Y, Babasaki T, Deguchi H, Hidaka A, Shimooka H and Takahashi S 2001 *Physica* E **9** 250
[22] Narath A and Barham D C 1973 *Phys. Rev.* B **7** 2195
[23] Dupree R, Walstedt R E and Warren W W Jr 1977 *Phys. Rev. Lett.* **38** 614
[24] Mukhamedshin I R, Alloul H, Collin G and Blanchard N 2005 *Phys. Rev. Lett.* **94** 247602
[25] Sakurai H, Takada K, Yoshii S, Sasaki T, Kindo K and Takayama-Muromachi E 2003 *Phys. Rev.* B **68** 132507
[26] Jin R, Sales B C, Li S and Mandrus D 2004 *Preprint* cond-mat/0410517

[27] Yosida K 1958 *Phys. Rev.* **110** 769
[28] Chou F C, Cho J H, Lee P A, Abel E T, Matan K and Lee Y S 2004 *Phys. Rev. Lett.* **92** 157004
[29] Yang H-B, Wang S-C, Sekharan A K P, Matsui H, Souma S, Sato T, Takahashi T, Takeuchi T, Campuzano J C, Jin R, Sales B C, Mandrus D, Wang Z and Ding H 2004 *Phys. Rev. Lett.* **92** 246403
[30] Tachiki M and Takahashi S 1989 *Solid State Commun.* **70** 291
[31] Mochizuki M, Yanase Y and Ogata M 2005 *J. Phys. Soc. Japan* **74** 1670
[32] Yanase Y, Mochizuki M and Ogata M 2004 private communications
[33] Fujimoto T, Zheng G, Kitaoka Y, Meng R L, Cmaidalka J and Chu C W 2004 *Phys. Rev. Lett.* **92** 047004
[34] Ishida K, Ihara Y, Kitagawa K, Murakawa H, Maeno Y, Michioka C, Kato M, Yoshimura K, Takada K, Sasaki T, Sakurai H and Takayama-Muromachi E 2003 *J. Phys. Soc. Japan* **72** 3041
[35] Higemoto W, Ohishi K, Koda A, Kadono R, Ishida K, Takada K, Sakurai H, Takayama-Muromachi E and Sasaki T 2004 *Phys. Rev.* B **70** 134508
[36] Boothroyd A T, Coldea R, Tennant D A, Prabhakaran D and Frost C D 2004 *Phys. Rev. Lett.* **92** 197201